

Excitation of parasitic waves near cutoff in forward-wave amplifiers

Gregory S. Nusinovich, Oleksandr V. Sinitsyn, and Thomas M. Antonsen, Jr.

Institute for Research in Electronics and Applied Physics, University of Maryland, College Park, Maryland 20742–3511, USA

(Received 7 June 2010; revised manuscript received 20 August 2010; published 25 October 2010)

In this paper, excitation of parasitic waves near cutoff in forward-wave amplifiers is studied in a rather general form. This problem is important for developing high-power sources of coherent, phase controlled short-wavelength electromagnetic radiation because just the waves which can be excited near cutoff have low group velocities. Since the wave coupling to an electron beam is inversely proportional to the group velocity, these waves are the most dangerous parasitic waves preventing stable amplification of desired signal waves. Two effects are analyzed in the paper. The first one is the effect of signal wave parameters on the self-excitation conditions of such parasitic waves. The second effect is the role of the beam geometry on excitation of these parasitic waves in forward-wave amplifiers with spatially extended interaction space, such as sheet-beam devices. It is shown that a large-amplitude signal wave can greatly influence the self-excitation conditions of the parasitic waves which define stability of operation. Therefore the effect described is important for accurate designing of high-power amplifiers of electromagnetic waves.

DOI: [10.1103/PhysRevE.82.046404](https://doi.org/10.1103/PhysRevE.82.046404)

PACS number(s): 52.59.Rz, 84.40.Fe, 84.40.Ik

I. INTRODUCTION

At present, there is a strong interest in increasing the power level of linear-beam amplifiers of coherent electromagnetic (EM) radiation at short wavelengths (W-band and above, up to the terahertz range). This interest is motivated by numerous civilian and military applications [1]. In order to increase the power level and/or the frequency range of microwave and millimeter-wave amplifiers, it is necessary to develop sources of coherent EM radiation with a spatially extended interaction space, i.e., operate at high-order modes/waves. Various concepts of millimeter-wave amplifiers with a spatially extended interaction space (sheet-beam traveling-wave tubes [2–5] and multiple-beam devices overviewed in Ref. [6]) are presently under study. One of the most critical issues in developing such amplifiers operating at high-order waves is excitation of parasitic waves. As a rule, especially dangerous are parasitic modes which can be excited at the ends of the passband [2]. Such waves have low group velocities and, hence, can be strongly coupled to the electron beam. Therefore they can be excited at lower currents than waves at frequencies far from cutoff. Excitation of waves near cutoff in backward-wave oscillators, i.e., in the absence of signal forward waves, was studied by a number of authors [7–10].

In this paper, we analyze the excitation of such waves in amplifiers, i.e., in the presence of a forward signal wave. A similar problem of excitation of parasitic waves in forward-wave amplifiers was studied in a rather general form in Ref. [11] where the analysis was, however, limited by parasitic waves operating far from cutoff. The excitation of parasitic waves in the presence of desired modes was also actively studied in oscillators operating at fast waves because such oscillators (cyclotron resonance masers [12], gyrotrons [13] and free-electron lasers [14]) can operate at very high-order modes with a dense spectrum of eigenfrequencies. Although below we restrict our consideration by amplifiers driven by linear electron beams, the same approach can be used for analyzing excitation of parasitic waves near cutoff (so-called gyrotron modes) in gyro-traveling-wave amplifiers (gyro-

traveling-wave tubes and gyrotrons) which are fast-wave amplifiers driven by beams of electrons gyrating in external magnetic field [12,13,15].

The excitation of parasitic waves near cutoff can take place in periodic slow-wave circuits with both, normal and anomalous dispersions. These two cases are illustrated by Fig. 1 where corresponding dispersion diagrams are shown; dispersion diagram of the operating and parasitic waves are

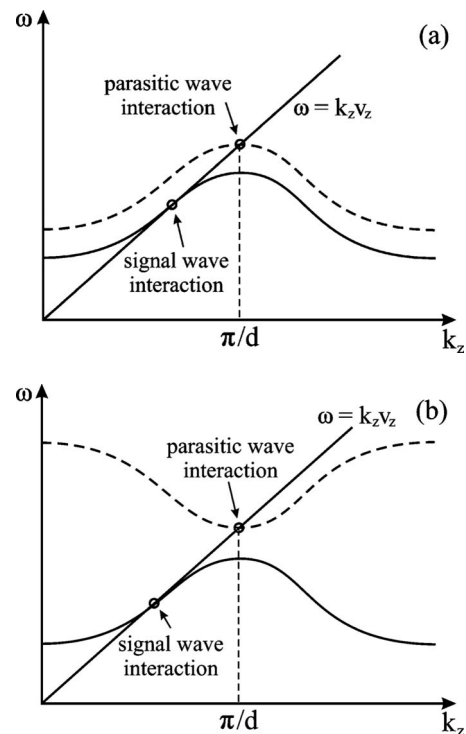


FIG. 1. Schematic of dispersion diagrams for the case when the parasitic mode has the normal (a) and anomalous (b) dispersion. The lower dispersion curve shows the signal wave, the upper one shows the parasitic mode. The straight line shows the beam line for the case of Cherenkov interaction of linearly moving electrons with the slow wave.

shown by the solid and dashed lines, respectively. Here ω , k_z , and d are the wave frequency, axial wave number and the circuit period, respectively. Straight line in Fig. 1 shows the beam line, i.e., the condition of Cherenkov synchronism $\omega = k_z v_z$ between the wave propagating with the phase velocity $v_{ph} = \omega/k_z$ and electrons with the velocity v_z . These diagrams are shown for the case when in the region of small axial wave numbers (from zero up to the π -point) the operating wave has normal dispersion, i.e., the frequency increases with the wave number. In such a case the group velocity $v_{gr} = d\omega/dk_z$ of the wave is positive and varies from zero (at $k_z=0$) to a certain positive value and then goes back down to zero at the π -point. Figures 1(a) and 1(b) correspond to the system with normal and anomalous dispersions of the parasitic wave, respectively. Most of the periodic slow-wave circuits (e.g., rippled-wall waveguides) have the normal dispersion. In the system with normal dispersion shown in Fig. 1(a), the dispersion diagram of the parasitic wave is similar to that of the operating wave. At the cutoff, i.e., at the π -point ($k_z d = \pi$), the group velocity $v_{gr} = d\omega/dk_z$ is zero, but its derivative $dv_{gr}/dk_z = d^2\omega/dk_z^2$ is nonzero and for the system with normal dispersion $dv_{gr}/dk_z < 0$. In the system with the anomalous dispersion (e.g., a coupled-cavity circuit) shown in Fig. 1(b), the dispersion diagram of the parasitic wave is different from that of the operating wave and at the π -point $dv_{gr}/dk_z > 0$.

Our paper is organized as follows. In Sec. II, we present the formulation of the problem under study. We distinguish here the cases of wave excitation far from cutoff and near cutoff. It is assumed that the signal wave is excited far from cutoff and operates in the stationary high-gain regime without reflections from the end of a well matched circuit. At the same time, the parasitic wave operating in the low-gain regime can be excited near cutoff. Details of formulation of the problem of such excitation are given below. In Sec. III, we present results of the study. In Sec. IV, we analyze the same problem in amplifiers with spatially extended interaction space. In Sec. V, we discuss the results obtained and in Sec. VI, we summarize the work.

II. FORMULATION

Since our goal is to derive and analyze the self-excitation conditions for the parasitic wave in the presence of the operating wave, we will assume that the amplitude of the parasitic wave is small in comparison with the signal wave amplitude and, hence, can be treated as a small parameter. Correspondingly, our treatment can be made in two steps. At the first step, we formulate equations describing the steady-state operation of the forward-wave amplifier, which is a well-studied problem. At the second step, we formulate equations describing the self-excitation of the parasitic wave in the presence of the large-amplitude signal wave. We will restrict our study by consideration of devices driven by low-voltage electron beams, i.e., equations for the electron motion will be treated in the nonrelativistic approximation. (Generalization of our formulation for the case of arbitrary electron energies can be done in a straightforward manner.) Prior to making the steps described above, let us analyze

some distinctions in the equations describing the device operation far from cutoff from that close to cutoff.

A. Wave excitation far and close to cutoff

Below we will neglect the space charge fields. Correspondingly, the electric and magnetic fields of the wave excited far from cutoff can be represented as

$$\vec{E} = \text{Re}\{A(z,t)\vec{E}_p(\vec{r}_\perp)e^{i(\omega t - k_z z)}\},$$

$$\vec{H} = \text{Re}\{A(z,t)\vec{H}_p(\vec{r}_\perp)e^{i(\omega t - k_z z)}\}, \quad (1)$$

where $A(z,t)$ is the slowly varying wave amplitude and $\vec{E}_p(\vec{r}_\perp)$ and $\vec{H}_p(\vec{r}_\perp)$ are the periodic eigenfunctions of the empty slow-wave structure defined in the same fashion as in Ref. [10].

By using the standard derivation technique described elsewhere [10] one can readily derive from Maxwell equations the wave equation for the wave whose fields are presented by Eq. (1),

$$\frac{\partial A}{\partial t} + v_{gr} \frac{\partial A}{\partial z} = -\frac{1}{U} \int_0^d dz \int_{S_\perp} \vec{j}_\omega \cdot \vec{E}_p^* e^{ik_z z} ds_\perp. \quad (2)$$

In Eq. (2), U is the microwave energy of the field with a unit amplitude stored in one period of the slow-wave structure and \vec{j}_ω is the Fourier component of the beam current density $\vec{j} = \text{Re}\{\vec{j}_\omega e^{i\omega t}\}$. This microwave energy contains contribution from all space harmonics of the periodic field, while in the electron interaction with the wave we will take into account the interaction with the synchronous harmonic only. (A role of nonsynchronous harmonics was analyzed elsewhere [16].) Taking into account the charge conservation law $j_z dt = j_0 dt_0$ and assuming a one-dimensional motion of electrons, Eq. (2) can be rewritten as

$$\frac{\partial A}{\partial t} + v_{gr} \frac{\partial A}{\partial z} = -\frac{1}{U} \int_0^d dz \int_{S_\perp} j_0 E_{pz}^* \left[\frac{1}{\pi} \int_0^{2\pi} e^{-i\omega t} d(\omega t_0) \right] e^{ik_z z} ds_\perp. \quad (2a)$$

In the case of steady-state operation the time derivative in the left-hand side of Eq. (2a) is zero.

The one-dimensional motion of nonrelativistic electrons can be described by the standard equation $dv_z/dt = -eE_z/m$ which in the case of steady-state operation can be rewritten in Lagrangian variables $t = t_0 + \int_0^z dz'/v_z$ as

$$\frac{\partial^2 t}{\partial z^2} = \frac{1}{v_z^3} \frac{eE_z}{m}. \quad (3)$$

Let us assume that the wave amplitude is relatively small and therefore the changes in the electron velocity are small, but the changes in the electron phase with respect to the signal wave $\theta = \omega t - k_z z$ can be significant. Then, in the right-hand side of Eq. (3) the electron velocity can be taken equal to its initial value v_{z0} , so

$$\frac{\partial^2 t}{\partial z^2} = \frac{1}{v_{z0}^3} \frac{eE_z}{m}. \quad (3a)$$

The electronic efficiency can be defined as

$$\eta = \frac{v_{z0}^2 - \langle v_z^2 \rangle}{v_{z0}^2} = \frac{2e}{mv_{z0}^2} \left\langle \int_0^L E_z dz \right\rangle. \quad (4)$$

Here angular brackets denote averaging over all initial distributions in the beam. Above, Eq. (2a) is written for the case when there is averaging over the electron entrance times and over the beam cross section.

It should be noted that when the wave group velocity is much smaller than the electron velocity, the characteristic time describing the evolution of the wave amplitude ($\tau_A \approx L/v_{gr}$) is much larger than the electron transit time ($T = L/v_{z0}$). In this case one can assume that the wave amplitude remains practically constant for a single electron transiting through the interaction space. Correspondingly, one can treat the electron motion assuming $A = \text{const}$, but take into account the slow evolution of the wave amplitude in Eq. (2a). Under this assumption one can derive from Eqs. (2a) and (4) the energy conservation law. To do this one should multiply Eq. (2a) by A^* , add to the equation obtained its complex conjugate and integrate over the interaction space. These steps result in the following equation describing slow temporal evolution of the microwave energy stored in the interaction space $W = (U/4d) \int_0^L |A|^2 dz$:

$$\frac{dW}{dt} + \frac{Uv_{gr}}{4d} \{ |A(L)|^2 - |A_0|^2 \} = P_b \eta. \quad (5)$$

In Eq. (5) $P_b = V_b I_b = I_b (mv_{z0}^2/2e)$ is the beam power, $|A_0|^2$ is the intensity of the signal wave entering the interaction space, while $|A(L)|^2$ characterizes the intensity of the outgoing radiation. This equation shows that the microwave energy stored in the interaction space increases when the power withdrawn from the beam [right-hand side (RHS) of Eq. (5)] exceeds the power flow from the structure. The second term in the left-hand side describes the microwave radiation losses. We can rewrite it in a standard form as $(\omega/Q)W$ and then, as follows from comparison of this term with Eq. (5) define the diffractive Q -factor as

$$Q = \frac{\omega}{v_{gr}} \frac{\int_0^L |A|^2 dz}{|A(L)|^2 - |A_0|^2}. \quad (6)$$

Certainly, such treatment is valid only in the case of strong reflections at the ends, when the circuit can be treated as a cavity.

In the case of the wave excited near cutoff we should consider the operation in the vicinity of the π -point where the group velocity is zero. In such a case, in the Taylor expansion of the wave dispersion characteristic one should take into account also the next term, i.e., represent the wave frequency as

$$\begin{aligned} \omega(k_z) = \omega(k_z - k_0) = \omega_0 + d\omega/dk_z|_{k_0}(k_z - k_0) \\ + (1/2)d^2\omega/dk_z^2|_{k_0}(k_z - k_0)^2, \end{aligned} \quad (7)$$

where ω_0 and k_0 are the frequency and axial wave number at the π -point where the first derivative of the frequency is zero. Correspondingly, as shown in Refs. [8,10], the wave Eq. (2a) should be replaced by the following one:

$$\begin{aligned} \frac{\partial A}{\partial t} - \frac{i}{2} \frac{d^2\omega}{dk_z^2} \Big|_{k_z=\pi/d} \frac{\partial^2 A}{\partial z^2} = -\frac{1}{U} \int_0^d dz \int_{S_\perp} j_0 E_{pz}^* \\ \times \left[\frac{1}{\pi} \int_0^{2\pi} e^{-i\omega t} d(\omega t_0) \right] e^{ik_z z} ds_\perp. \end{aligned} \quad (8)$$

Repeating the steps described above one can derive a corresponding equation describing the temporal evolution of the microwave energy stored in the interaction space,

$$\begin{aligned} \frac{dW}{dt} + \frac{U}{4d} \frac{d^2\omega}{dk_z^2} \Big|_{k_z=\pi/d} \left\{ \text{Im} \left(A^* \frac{\partial A}{\partial z} \right) \Big|_{z=L} - \text{Im} \left(A^* \frac{\partial A}{\partial z} \right) \Big|_{z=0} \right\} \\ = P_b \eta. \end{aligned} \quad (9)$$

Accurate analysis of the boundary conditions for the wave amplitude and its derivative at both ends was carried out elsewhere [8,10]. In particular, in Ref. [10] it was explained how the boundary conditions at both ends of the circuit should be determined. Without going into details of this procedure, let us only point out that the second term in the LHS of Eq. (9) can again be treated as $(\omega/Q)W$. This results in the following definition of the diffractive Q -factor for modes excited near cutoff,

$$Q = \frac{\omega}{\frac{d^2\omega}{dk_z^2} \Big|_{k_z=\pi/d} \frac{\int_0^L |A|^2 dz}{\text{Im} \left(A^* \frac{\partial A}{\partial z} \right) \Big|_{z=L} - \text{Im} \left(A^* \frac{\partial A}{\partial z} \right) \Big|_{z=0}}}. \quad (10)$$

Then, Eq. (9) can be rewritten as

$$\frac{dW}{dt} + \frac{\omega}{Q} W = P_b \eta \quad (11)$$

and the self-excitation of this wave near cutoff can be written in a standard form as

$$P_b \eta > \frac{\omega W}{Q}. \quad (12)$$

Equation (12) tells that for exciting the microwave oscillations the power withdrawn from the beam should exceed the power of microwave losses.

It can be instructive to compare the definition of Q given by Eq. (10) with the diffractive Q of gyrotron cavities where the role of cavities is played by slightly irregular smooth-wall open waveguides excited near cutoff [17]. In such waveguides, the dependence of the wave frequency on the

axial wave number is simple: $\omega = \sqrt{\omega_{cut}^2 + c^2 k_z^2}$. Correspondingly, its second derivative is $d^2\omega/dk_z^2|_{\omega_{cut}} = c^2/\omega_{cut}$. Also, one can assume that the gyrotron cavity is bounded at the cathode side by the cutoff narrowing, i.e., $A(0)=0$, while at the cavity output the radiation condition $\frac{\partial A}{\partial z}|_{z=L} = ik_z A(L)$ holds where for the mode with one axial variation the axial wave number is $k_z \approx \pi/L$. Substituting these formulas in Eq. (10) we get $Q_{dif} \approx 4\pi(L/\lambda)^2$ which is the known definition of the minimum diffractive Q -factor for gyrotron cavities [13,17].

B. Large-signal theory of the forward-wave amplifier

Below we will denote all variables related to the signal wave by the subindex “1” and later, when we will consider the parasitic wave, that wave will be denoted by the subindex “2.” In this subsection we will consider the steady-state operation, i.e., neglect time derivatives. Introducing $\theta_1 = \omega_1(t - z/v_{z0})$, normalized axial coordinate $\xi = z/L$ (L is the interaction length), electron transit angle $\Theta_1 = (\omega_1/v_{z0} - k_{z1})L = (\omega_1 - k_{z1}v_{z0})T$, the normalized wave amplitude $\bar{A}_1 = (\omega_1 T / \beta_{z0}^2)(eA_1 L / mc^2)$ and the normalized beam current parameter $I_1 = (eI_b / mc^3)(\omega_1 T / \beta_{z0}^2 \beta_{gr})(dL^2 / U_1)$ allows us to rewrite equation for electron motion [Eq. (3a)] and the wave Eq. (2a), respectively, as

$$\frac{\partial^2 \theta_1}{\partial \xi^2} = \text{Re}\{\bar{A}_1 E_{1z} e^{i(\theta_1 + \Theta_1 \xi)}\}, \tag{13}$$

$$\frac{\partial \bar{A}_1}{\partial \xi} = I_1 \frac{1}{S_b} \int_{S_\perp} \Psi E_{1z}^* ds_\perp \left[\frac{1}{\pi} \int_0^{2\pi} e^{-i(\theta_1 + \Theta_1 \xi)} d\theta_{10} \right]. \tag{14}$$

This pair of equations forms a self-consistent set describing the steady-state amplification of the signal wave in an amplifier with an arbitrary transverse cross section of a waveguide and arbitrary cross-section of an electron beam. In transforming Eq. (2a) into Eq. (14) the electron current density was represented as $j_0 = -(I_b/S_b)\Psi(\vec{R}_b)$ where I_b is the beam current in Amperes, S_b is the electron beam cross-sectional area and the function $\Psi(\vec{R}_b)$ describes the electron current density distribution over the cross section; the normalization condition for this function is $\int_{S_\perp} \Psi(\vec{R}_b) ds_\perp = S_b$.

When all electrons interact with the wave of the same amplitude, i.e., the function $E_{1z}(\vec{R}_b)$ for all electrons is the same, we can introduce $\hat{A}_1 = \bar{A}_1 E_{1z}(\vec{R}_b)$ and $\hat{I}_1 = I_1 |E_{1z}(\vec{R}_b)|^2$. In the equations derived from Eqs. (13) and (14) with these notations a new normalized beam current parameter plays the role of the Pierce gain parameter. So, denoting \hat{I}_1 by C_1^3 , introducing the normalized axial coordinate $\varsigma = C_1 \xi$ and the wave amplitude $\alpha_1 = (\hat{A}_1 / C_1^2) \exp(i\Theta_1 \xi)$ we can reduce Eqs. (13) and (14) to the following set of equations containing the minimal number of parameters:

$$\frac{\partial^2 \theta_1}{\partial \varsigma^2} = \text{Re}\{\alpha_1 e^{i\theta_1}\}, \tag{15}$$

$$\frac{\partial \alpha_1}{\partial \varsigma} - i\delta_1 \alpha_1 = \frac{1}{\pi} \int_0^{2\pi} e^{-i\theta_{10}} d\theta_{10}. \tag{16}$$

In Eqs. (16) we introduced the detuning $\delta_1 = \Theta_1 / C_1$ which is identical to the velocity parameter b used by Pierce. In the presence of the wave attenuation, the wave number is complex and, hence, this parameter also contains the imaginary part. The boundary conditions for Eqs. (15) and (16) should be given at the entrance $\varsigma=0$: $\theta_1(0) = \theta_{10} \in (0; 2\pi]$, $\partial\theta_1/\partial\varsigma|_0 = 0$, and $\alpha_1(0) = \alpha_{10}$. The electronic efficiency [Eq. (4)] can be represented as $\eta = (2C_1/\omega_1 T) \hat{\eta}$ where we introduced the normalized efficiency

$$\hat{\eta} = \frac{1}{2\pi} \int_0^{2\pi} \frac{\partial \theta_1}{\partial \varsigma} d\theta_{10}. \tag{17}$$

Equations (15)–(17) were first formulated by Weinstein in his one-dimensional nonlinear theory of the traveling-wave tube [18]; results of their studies are essentially the same as those by Nordsieck [19]. Later, the same equations were used for studying nonlinear theory of ubitrons [20] and free-electron lasers [14].

Repeating the steps described in deriving Eq. (5) above one can derive from Eqs. (15)–(17) the energy conservation law in a simple form:

$$|\alpha_1|^2 - |\alpha_{10}|^2 = 4\hat{\eta}. \tag{18}$$

C. Self-excitation of the parasitic wave in the presence of the signal wave

Assume that the amplitude of the parasitic wave is small and therefore its effect on the electron motion can be treated as a small perturbation. Then, in the equation for electron motion [Eq. (3a)], in the case when an electron interacts with two waves and $|A_2| \ll |A_1|$, we can represent the electron time variable as $t = t_{(1)} + t_{(2)}$. Here the first term $t_{(1)}$ describes the effect of the first wave and the corresponding equation was transformed into Eqs. (13) and (15) above. The second term $t_{(2)}$ describes the effect of the second wave. A corresponding equation for electron motion follows from Eq. (3a) which, being linearized with respect to $|A_2|$, can be written as

$$\frac{\partial^2 t_{(2)}}{\partial z^2} = \frac{1}{v_{z0}^3} \frac{e}{m} \text{Re}\{A_2 E_{2pz}(\vec{R}_b) \exp[i(\omega_2 t_{(1)} - k_{z2} z)]\}, \tag{19}$$

where the phase factor in the RHS can be rewritten as $\omega_2 t_{(1)} - k_{z2} z = (\omega_2/\omega_1)\theta_1 + [\Theta_2 - (\omega_2/\omega_1)\Theta_1]z$. Correspondingly, in the RHS of Eq. (8) the exponential term can be represented as $\exp(-i\omega_2 t) \approx \exp(-i\omega_{(2)} t_{(1)}) (1 - i\omega_2 t_{(2)})$. After averaging over the electron entrance phases in Eq. (8) only the last term proportional to $t_{(2)}$ is there nonzero. This reduces Eq. (8) to

$$\begin{aligned} \frac{\partial \bar{A}_2}{\partial t} + i\Omega'' \frac{\partial^2 \bar{A}_2}{\partial \xi^2} = & -iI_2 \frac{1}{S_b} \int_{S_\perp} \Psi E_{2z}^* ds_\perp \\ & \times \left[\frac{1}{\pi} \int_0^{2\pi} (t_{(2)}) e^{-i\Phi} d\theta_{10} \right]. \end{aligned} \tag{20}$$

In Eq. (20), we introduced $\Omega'' = \partial^2 \omega_2 / \partial k_{z2}^2|_{k_{z2} = \pi_d / 2\beta_{z0} cL}$, nor-

malized time $t' = t/T$ [in Eq. (20) the prime is omitted] and the beam current parameter $I_2 = (eI_b/mc^3)(\omega_2 T d L^2 / U_2 \beta_{z0}^3)$ which is similar to that of the signal wave in Eq. (14). We also used the notation $\Phi = (\omega_2 / \omega_1) \theta_1 + [\Theta_2 - (\omega_2 / \omega_1) \Theta_1] \xi$.

When all electrons are equally coupled to the parasitic wave, we can reduce Eqs. (19) and (20) to the following set:

$$\frac{\partial^2 t_{(2)}}{\partial \xi^2} = \text{Re}\{\hat{A}_2 e^{i\Phi}\}, \quad (21)$$

$$\frac{\partial \hat{A}_2}{\partial t} + i\Omega'' \frac{\partial^2 \hat{A}_2}{\partial \xi^2} = -iI_2 \left[\frac{1}{\pi} \int_0^{2\pi} t_{(2)} e^{-i\Phi} d\theta_{10} \right]. \quad (22)$$

These equations yield the energy conservation law which can be written in the following form:

$$\frac{dW_2}{dt} + P_{loss} = -2I_2 \left[\frac{1}{\pi} \int_0^{2\pi} \int_0^{\xi_{out}} t_{(2)} \text{Im}\{\hat{A}_2 e^{i\Phi}\} d\xi d\theta_{10} \right]. \quad (23)$$

Here the second term in the left-hand side represents all sorts of losses: $P_{loss} = P_\Omega + P_L + P_R$ where $P_\Omega = (\omega / Q_\Omega) W_2$ describes the Ohmic losses in the circuit and two other terms describe the wave power flow through the left ($\xi=0$) and right ($\xi=\xi_{out}$) cross sections, respectively. When Ohmic losses are negligibly small and the waveguide on the left (cathode side) is below cutoff for the parasitic wave the loss power is equal to $P_{loss} = P_R = 2\Omega'' h_2 L |\hat{A}_2(\xi=1)|^2$. Here the deviation of axial wave number about the π -point h should match the sign of the second derivative of the frequency in order to give the positive value of the power flow out from the circuit. It is obvious that the self-excitation of the parasitic mode takes place when the power withdrawn by the second mode from the beam [RHS of Eq. (23)] exceeds the power of microwave losses. Correspondingly, the self-excitation condition of the second mode, for example, in the case of only diffractive losses via the output cross section can be written as

$$-\hat{I}_2 \left[\frac{1}{\pi} \int_0^{2\pi} \int_0^{\xi_{out}} t_{(2)} \text{Im}\{\hat{A}_2 e^{i\Phi}\} d\xi d\theta_{10} \right] > \Omega'' h_2 L |\hat{A}_2(\xi=1)|^2. \quad (24)$$

Since the entrance and exit cross sections of the circuit are not matched for the parasitic wave we can assume that there are strong reflections of the waves forming this mode from both ends and therefore these waves form a mode with the standing pattern. So the amplitude of this mode can be presented as $\hat{A}_2 = A_2(t) f_2(\xi)$ that allows us to rewrite the self-excitation condition in variables normalized to the Pierce gain parameter of the signal wave ($\varsigma = C_1 \xi$, $\alpha_2 = \hat{A}_2 / C_1^2$, $\tau = C_1(t/T)$, and $\mu = C_1 \Omega''$) as follows:

$$G_2 \geq |f_2(\varsigma_{out})|^2 \frac{|E_{1z}(\vec{r}_b)|^2 U_2 \omega_1}{|E_{2z}(\vec{r}_b)|^2 U_1 \omega_2 \beta_{g1}} \left| h_2 \frac{d\beta_{g2}}{dh_2} \right|_{h_{20}}. \quad (25)$$

Here the right-hand side contains the ratio of parameters characterizing the beam coupling to the waves and the en-

ergy propagation of both waves through the circuit. Also in Eq. (25) the function

$$G_2 = -2 \text{Im} \left\{ \frac{1}{2\pi} \int_0^{2\pi} \left[\int_0^{\varsigma_{out}} f_2 e^{i(\delta_2 \varsigma + \theta_1)} \times \left(\int_0^\varsigma \int_0^{\varsigma'} f_2^* e^{-i(\delta_2 \varsigma'' + \theta_1)} d\varsigma'' d\varsigma' \right) d\varsigma \right] d\theta_{10} \right\} \quad (26)$$

describes the interaction of the beam modulated by the signal wave with the parasitic mode and can be called the gain function of the second mode in the presence of the signal wave. In Eq. (26), the phase θ_1 is the electron phase with respect to the phase of the signal wave defined by Eq. (15) above and $\delta_2 = \Theta_2 / C_1$ is the detuning of the second mode normalized to the Pierce gain parameter of the signal wave. Performing integration by parts one can rewrite Eq. (26) in a more compact form as

$$G_2 = \frac{\partial}{\partial \delta_2} \frac{1}{2\pi} \int_0^{2\pi} \left\{ \left| \int_0^{\varsigma_{out}} f_2 e^{i(\delta_2 \varsigma + \theta_1)} d\varsigma \right|^2 \right\} d\theta_{10}. \quad (27)$$

Equation (27) contains the derivative of the spectral intensity of the EM force acting upon electrons, so it indicates that in a certain sense our system has the gain function property referred to as Madey's theorem [21]. Note that quite similar is the expression defining the beam-loading conductance in linear-beam klystrons in the kinematic approximation [22]. As known, the negative value of this conductance determines so-called monotron instability [22,23]. Our case under study is specific in the sense that here the gain function of the second mode depends on the electron interaction with the first mode.

III. RESULTS

A. Signal wave operation

In this section we present some results illustrating the amplification of the signal wave in the stationary regime. These results are identical to well known results of the one-dimensional nonlinear theory of the TWT in Pierce parameters [18] and are given here just for completeness of the study. In Fig. 2, the axial dependence of the wave amplitude is shown for three initial values: $\alpha_{10} = 0.001, 0.01$ and 0.1 . Figures 2(a)–2(c) correspond to different values of the detuning $\delta_1: 0, -1.0$ and 1.0 . As one can see, the distance at which the device reaches the saturation shortens as the input amplitude increases. When the system reaches the saturation the maximum normalized efficiency [Eq. (17)] practically does not depend on the initial amplitude (when this amplitude is small enough), but strongly depends on the detuning. In Fig. 3, this maximum normalized efficiency $\hat{\eta}$ is shown as the function of the detuning δ_1 .

B. Effect of the signal wave on the self-excitation condition of the parasitic mode

We analyzed the self-excitation of the second mode assuming that this mode is formed by the superposition of the forward and backward waves operating in a low-gain regime

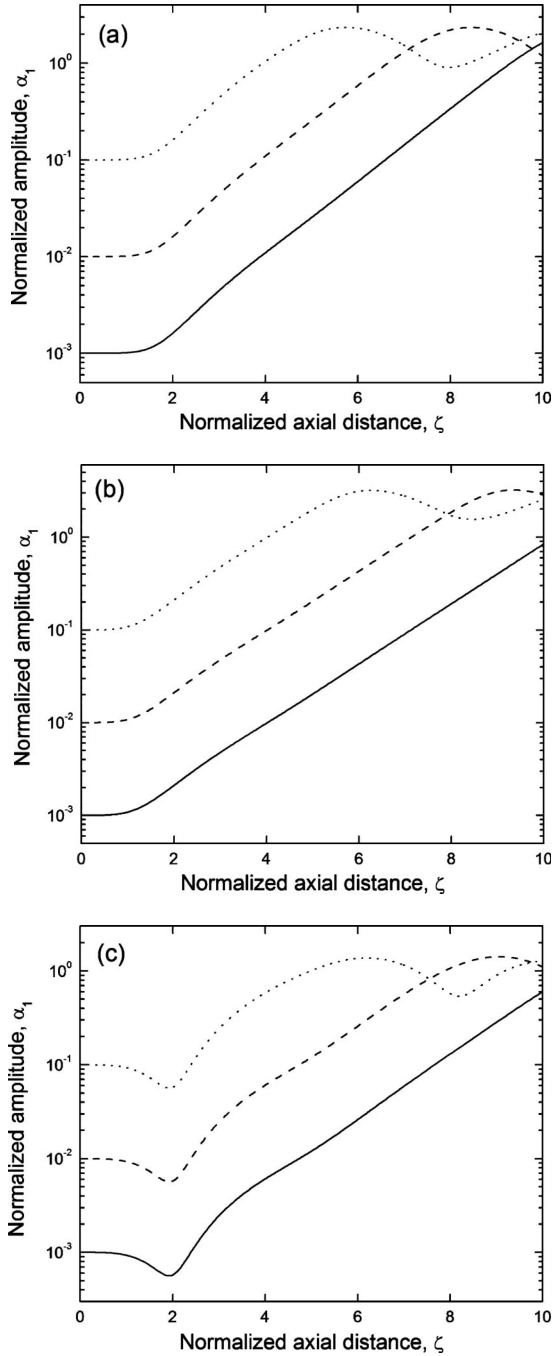


FIG. 2. Axial dependence of the signal wave amplitude for several values of the detuning between the signal wave and electrons: (a) $\delta_1=0$, (b) $\delta_1=-1.0$, (c) $\delta_1=1.0$.

in a circuit with strong end reflections. The wave amplitude in the low-gain regime varies slightly along the device axis, so, due to the strong reflections these two waves have almost constant amplitudes along the axis. The backward wave with the axial wave number $k_z \approx -\pi/d$ is far from synchronism and therefore does not contribute significantly to the energy exchange with electrons [16], so it can be ignored. However, the forward-wave component propagating in z -direction with the axial wave number $k_z \approx \pi/d$ (d is the structure period) is synchronous with electrons and should be considered accurately. When the beam line intersects the dispersion curve of

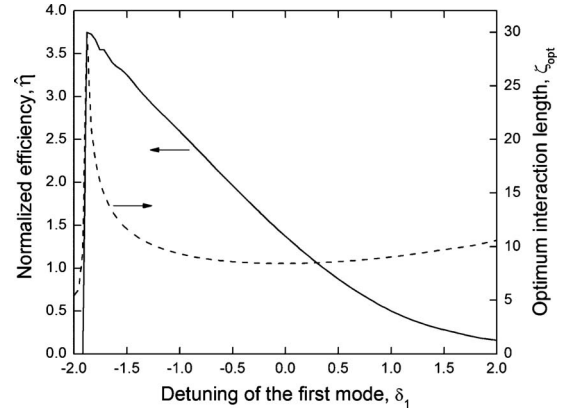


FIG. 3. The maximum normalized efficiency (solid line) and the optimum interaction length (dashed line) as functions of the detuning δ_1 . The optimal length is shown for the initial wave amplitude equal to $\alpha_{10}=0.01$. At smaller amplitudes the optimal length is larger and the break of the field in the region of large absolute values of the detuning δ_1 (in the left part of the figure) occurs at smaller detunings $|\delta_1|$.

a SWS in the vicinity of the π -point, its axial wave number can be written as $k_z = \pi/d + \Delta k_z$. In the vicinity of this intersection point also the wave of the same frequency with $k_z = \pi/d - \Delta k_z$ exists. When $|\Delta k_z|L \leq 2\pi$, such a wave synchronously interacts with electrons. The wave with $\Delta k_z > 0$, which is located in the dispersion diagram shown in Fig. 1 on the right from the π -point has a negative group velocity, while the wave with $\Delta k_z < 0$ located on the left has a positive one. The axial structure of the parasitic wave consisting of these two can be given in Eqs. (26) and (27) as $f(s) = (1/2)(1 + \cos \Delta s)$ where $\Delta = 2\Delta k_z L / C_1$. In the case of $\Delta = 0$ this function is equal to 1.

The effect of the signal wave on the excitation of the parasitic mode with such axial structure is illustrated by the results shown in Figs. 4 and 5. In Figs. 4(a)–4(c) the gain function G_2 given by Eqs. (26) or (27) characterizing the self-excitation conditions of the parasitic mode is shown as the function of the detuning δ_2 for $\Delta = 0$ and several values of the detuning of the signal wave: (a) $\delta_1 = 0$, (b) $\delta_1 = 0.5$, and (c) $\delta_1 = 1.0$. The interaction distance in all the cases shown in Fig. 4 is equal to $s_{out} = 10$. Figure 4(d) illustrates the effect of departure of operation from the π -point. Clearly this departure weakens the gain function of the second mode. Solid, dashed, and dotted lines in figures (a)–(c) correspond to the initial amplitudes equal to 0.001, 0.005, and 0.01, respectively. At small values of the initial amplitude this function is practically the same as in the absence of the signal wave (cf. Fig. 4.2 in Ref. [14]; the difference in the absolute values of the gain function is due to different normalizations of the function describing the axial structure of the field). As the initial value of the signal wave amplitude increases, the peak of this gain function G_2 , as seen in Fig. 4, becomes much smaller that corresponds to the suppression of the parasitic mode. When the interaction distance is shorter, significant deformation of the gain curves for the parasitic mode takes place at larger values of the input amplitude of the signal wave. For example, in the case of $s_{out} = 5$ (not shown here) the gain curves for initial amplitudes of the signal wave

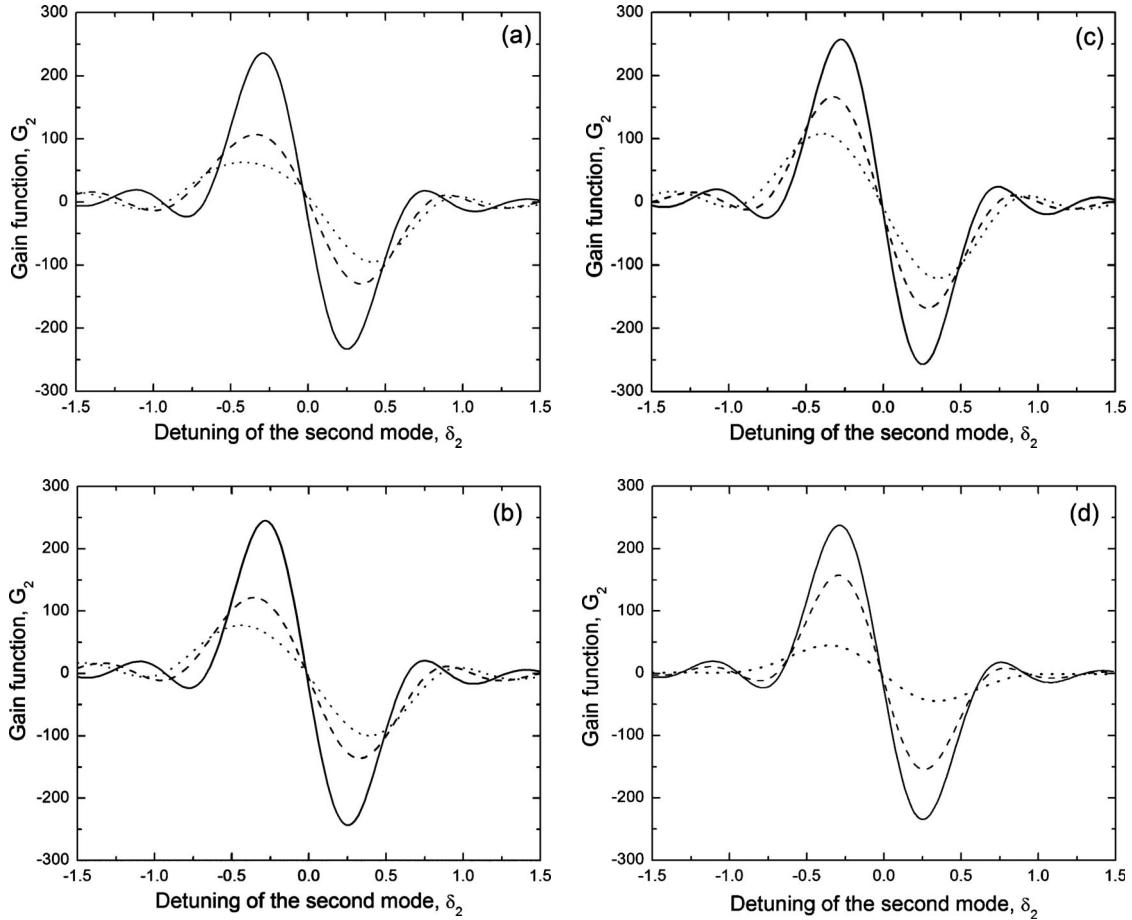


FIG. 4. The gain function of the second mode as the function of the second mode detuning δ_2 for several values of the signal amplitude at the entrance and different values of the detuning between the signal wave and electrons: (a) $\delta_1=0$, (b) $\delta_1=0.5$, (c) $\delta_1=1.0$. Figure 4(d) illustrates the effect of the departure of the operating point from the π -point. Solid, dashed and dotted lines corresponds to $\Delta=0$, $\pi/20s_{out}$ and $\pi/10s_{out}$, respectively. The normalized length is equal to $s_{out}=10$.

equal to 0.001 and 0.01 are practically identical, but their deformation becomes significant when the input amplitude is close to 0.1. So in this regard the system under consideration behaves very similar to the gyrotron where the effect of suppression of the parasitic mode by the first excited operating mode was shown elsewhere [24,25].

It should also be noted that in the region of small detunings δ_2 (less than about $-0.5-0.6$) the value of the gain function G_2 increases with the initial amplitude of the signal wave. This indicates that in this region of the detunings another effect known as the nonlinear mode excitation [25] or the cross-excitation instability [26,27] takes place. The nonlinear mode excitation means that the presence of one mode lowers the start current of another mode just making its excitation possible in the region where this mode could not be excited in the absence of the first mode.

Contours of equal values of the gain function G_2 in the plane of detunings of two modes are shown in Fig. 5 for the normalized interaction length equal to $s_{out}=5$ and several values of the initial amplitude of the signal wave. Figures (a), (b), and (c) show contours of the gain function equal to 1.0, 6.0, and 10.0, respectively. So these contours determine the regions of excitation of the parasitic mode in the case of corresponding ratios of the coupling impedances of the beam

to both waves given by the condition of self-excitation [Eq. (25)]. Black, red, green, and blue lines correspond to initial amplitudes of the signal wave equal to 0.01, 0.1, 0.2, and 0.25, respectively. At small amplitudes the lines of the gain function do not depend on the frequency detuning of the signal wave, which indicates that the signal wave has practically no effect on the condition of excitation of the parasitic mode. For example, in the case shown in Fig. 5(a), the region of parasitic mode self-excitation at so small input amplitude occupies the range of detunings of the second mode from -1.23 to about 0. Also, another region of excitation takes place at the detuning smaller than -1.87 where another peak of the gain function of the parasitic mode exists. Contours of larger values of the parasitic mode gain function have slightly different boundaries [cf. Figs. 5(a)–5(c)].

The increase in the input amplitude of the signal wave causes deformation of these contours as shown in Fig. 5. First, when the input amplitude increases from 0.01 to 0.1 these contours in all figures deform to the left in the region of the signal wave detunings close to zero, i.e., in the middle of the amplification region of the signal wave. Then, contours of larger values of the parasitic mode gain function [see Fig. 5(c)] exhibit more complicated deformation: when the input amplitude of the signal wave equals 0.2 the left contour

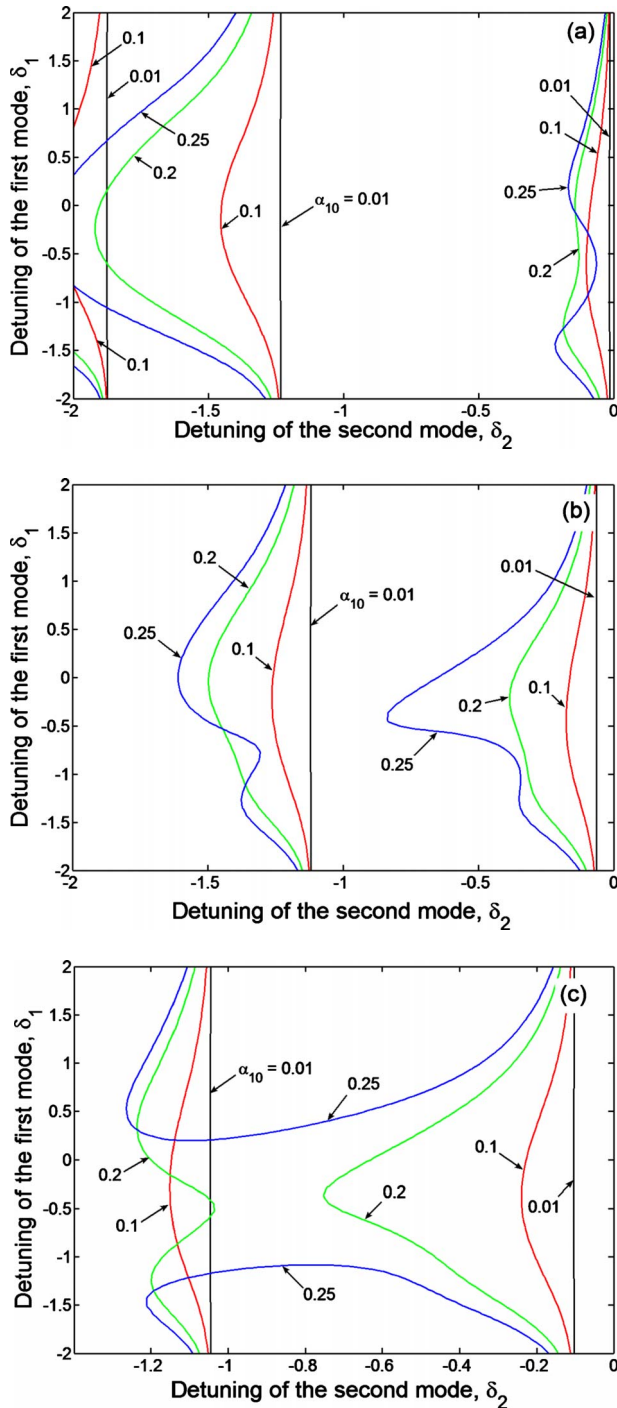


FIG. 5. (Color online) Contours of equal values of the gain function of the second mode [(a) $G_2=1.0$, (b) $G_2=6.0$ and (c) $G_2=10.0$] in the plane of detunings δ_1 versus δ_2 for several values of the signal wave amplitude at the entrance: $\alpha_{10}=0.01$ (black solid lines), 0.1 (red dashed lines), 0.2 (green dotted lines) and 0.25 (blue dash-dotted lines). The normalized length is equal to $s_{out}=5.0$.

has a peak moving to the right, while the right contour rapidly moves to the left. With the further increase in α_{10} these contours merge and, as shown in Fig. 5(c) for $\alpha_{10}=0.25$ (blue lines), the region of the parasitic mode gain function larger than 10.0 does not exist in the middle of the signal wave amplification zone. This deformation clearly demonstrates

the effect of suppression of the parasitic mode by the signal wave. Quite similar deformation takes place for the contours $G_2=7.0$ (not shown here), but the tendency weakens for contours of the smaller values of this gain function.

For example, contours of $G_2=1.0$ shown in Fig. 5(a) show that the deformation of the right boundary with the increase in α_{10} is not as strong as the deformation of the left boundary. As the result, the region of excitation of the parasitic mode in the case of equal coupling impedances of both waves to the beam [see the right-hand side of Eq. (25)] expands that indicates that in this case the effect of nonlinear mode excitation dominates. In general, results shown in Fig. 5 clearly demonstrate that the self-excitation conditions of such parasitic waves in amplifiers operating in large-signal regimes cannot be correctly estimated without account for the effect of the signal wave on the parasitic mode.

IV. EXCITATION OF PARASITIC MODES IN SYSTEMS WITH A SPATIALLY EXTENDED INTERACTION SPACE

Above, we analyzed interaction between the waves equally coupled to all beam electrons. As discussed in Introduction, for increasing the power of EM radiation it is necessary to develop devices with a spatially extended interaction space. This is why in recent years so much attention was paid to such concepts as multiple-beam and sheet-beam configurations; proper references to original contributions on multiple-beam klystrons can be found in [28,22,6], sheet-beam traveling wave tubes and sheet-beam klystrons had been studied, respectively, in [4,5] and [23,29] (see also references therein).

One of the effects occurring in high-power sources of EM radiation with spatially extended interaction space which was absent in conventional systems having cylindrical symmetry is the coupling between modes. Indeed, as a rule, the EM fields of empty circuits are described by a set of orthogonal nondegenerate functions. Therefore, in the presence of an electron beam having the same symmetry, the normal modes of such devices remain orthogonal. This means that when the amplitude of EM fields is small each of them can be excited independently on others. At large amplitudes the nonlinear effects lead to the coupling between modes and this coupling is usually interpreted as the mode or wave interaction. Above, we considered the effect of the signal wave operating in the large-signal regime on the parasitic mode assuming that all electrons are equally coupled to each of these modes. Now we will analyze the effect of the difference in the coupling of an extended electron beam to these modes.

In a steady-state regime the amplification of the signal wave by a spatially extended electron beam can be described by Eqs. (13) and (14). Correspondingly, the excitation of the parasitic wave can be described by Eqs. (19) and (20). In both sets of equations, the transverse structures of axial components of the wave fields, which are given by functions E_{1z} and E_{2z} , respectively, in the region occupied by the beam is now important.

Let us restrict our study by a simple example of a one-dimensional nonuniformity in one of transverse directions.

Assume that an electron beam with a given value of the beam current is infinitely thin in y -direction and uniformly distributed in x -direction from $-L_{bx}/2$ to $+L_{bx}/2$. Also assume that the spatial distribution of axial components of the signal wave and the parasitic mode in the x -direction can be approximated by the functions $\psi_{1,2} = \cos(q_{1,2}\pi K\hat{x}/2)$, respectively. Here the mode indices are not equal, $q_1 \neq q_2$, the transverse coordinate is normalized to the beam width, $\hat{x} = 2x/L_{bx}$ and the parameter $K = L_{bx}/L$ is the ratio of the beam width L_{bx} to the width of a circuit L . This parameter can be treated as the filling factor. Then, the amplification of the signal wave can be described, instead of Eqs. (15) and (16), by the following equations:

$$\frac{\partial^2 \theta_1}{\partial s^2} = \text{Re} \left\{ \alpha_1 e^{i\theta_1} \cos\left(q_1 \frac{\pi}{2} K\hat{x}\right) \right\}, \quad (28)$$

$$\frac{\partial \alpha_1}{\partial s} - i\delta_1 \alpha_1 = \frac{1}{\pi} \int_0^{2\pi} \left\{ \frac{1}{2} \int_{-1}^{+1} e^{-i\theta_1} \cos\left(q_1 \frac{\pi}{2} K\hat{x}\right) d\hat{x} \right\} d\theta_{10}. \quad (29)$$

Correspondingly, the normalized efficiency can be defined instead of Eq. (17) as

$$\hat{\eta} = \frac{1}{2} \int_{-1}^{+1} \left\{ \frac{1}{2\pi} \int_0^{2\pi} \frac{\partial \theta_1}{\partial s} d\theta_{10} \right\} d\hat{x}. \quad (30)$$

Similarly, the gain function of the second mode, instead of Eq. (27), can be defined as

$$\langle G_2 \rangle = \frac{1}{2} \int_{-1}^{+1} G_2 d\hat{x}, \quad (31)$$

where the function G_2 is defined by Eq. (27) in which the function $f_2(s)$ describing the axial structure of the mode should be replaced by the function $f_2(s)\psi_2(\hat{x})$ which is the product of two functions describing both the axial and transverse distributions of the parasitic mode.

The effect of the filling factor K on the normalized efficiency of the signal wave is illustrated by Fig. 6 where this efficiency is shown as the function of the frequency detuning δ_1 . Here and below we consider the signal wave with one variation in the transverse direction $q_1 = 1$. Figures (a) and (b) correspond to different initial amplitudes of the wave. The peaks of these curves are displaced in the region of negative detunings in accordance with results shown in Fig. 3 and, as the input amplitude increases, this displacement becomes larger. At low input power level [see Fig. 6(a) where $\alpha_{10} = 0.1$], as the filling factor increases, these peaks decrease. This effect can be explained by the fact that at low initial amplitudes the wave growth doesn't reach saturation (cf. results shown in Fig. 2). Therefore expansion of the beam in the region of lower coupling to the wave lowers the growth rate of a whole beam even further that results in the efficiency degradation. At larger initial amplitudes [see Fig. 6(b) where $\alpha_{10} = 0.25$] the wave growth saturates and even more, in a certain range of detunings, the efficiency starts decreasing at the end due to electron overbunching. Correspondingly, in this range of detunings located to the right from the optimal one, the beam widening mitigates the effect of over-

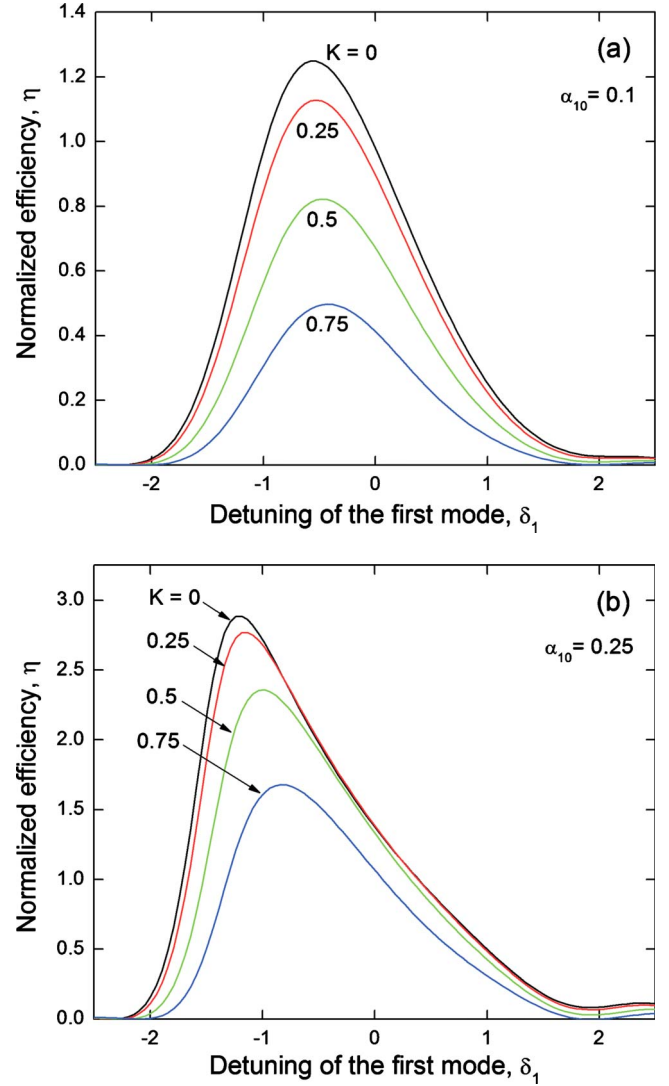


FIG. 6. (Color online) Effect of the beam widening on the efficiency of the signal wave at different values of the initial amplitude: (a) $\alpha_{10} = 0.1$, (b) $\alpha_{10} = 0.25$. The normalized interaction length equals to 5.0.

bunching and, as a result the efficiency becomes approximately equal at different values of the filling factor [cf. curves for $K=0.0$, $K=0.25$ and $K=0.5$ in Fig. 6(b)].

The effect of the beam widening on the excitation of the second mode is illustrated by Figs. 7 and 8. In Fig. 7, the gain function of the second mode is shown as the function of the second mode detuning δ_2 in figures (a), (b), and (c) for the cases when this mode has one, two, and three variations, respectively. These figures are plotted for specific values of the input amplitude and detuning of the signal wave ($\alpha_{10} = 0.01$, $\delta_1 = -0.5$) and different values of the filling factor. Clearly, in all three figures the curves for a pencil beam ($K = 0$) are the same. In the first case ($q_2 = 1$) shown in Fig. 7(a), the transverse structure of the second mode is the same as that of the signal wave. Therefore the transverse expansion of the beam causes gradual lowering of the peak of the gain function because the beam coupling to the parasitic wave averaged over the beam cross-section becomes smaller.

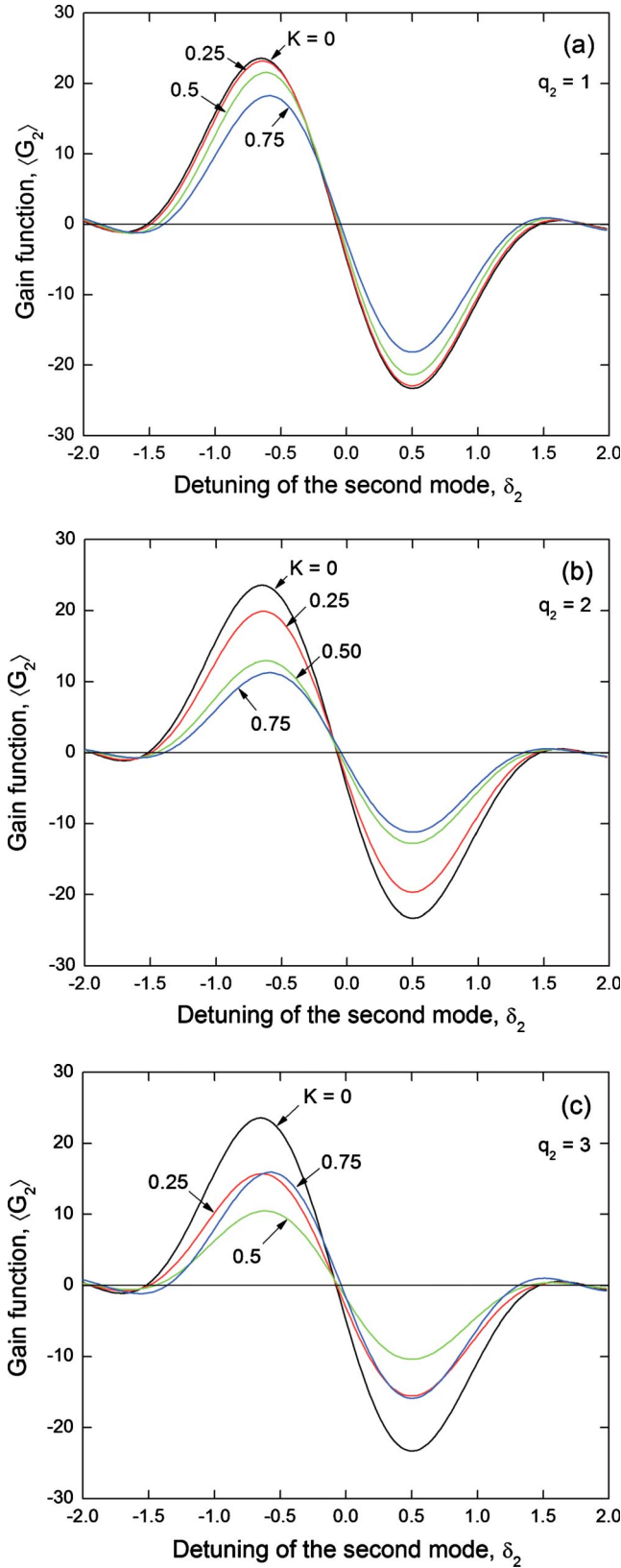


FIG. 7. (Color online) Gain function of the parasitic mode as the function of its detuning for different values of the beam filling factor in the cases of modes with different transverse indices: (a) $q_2=1$, (b) $q_2=2$, (c) $q_2=3$. Results are shown for the input amplitude of the signal wave $\alpha_{10}=0.1$ and its detuning $\delta_1=0$.

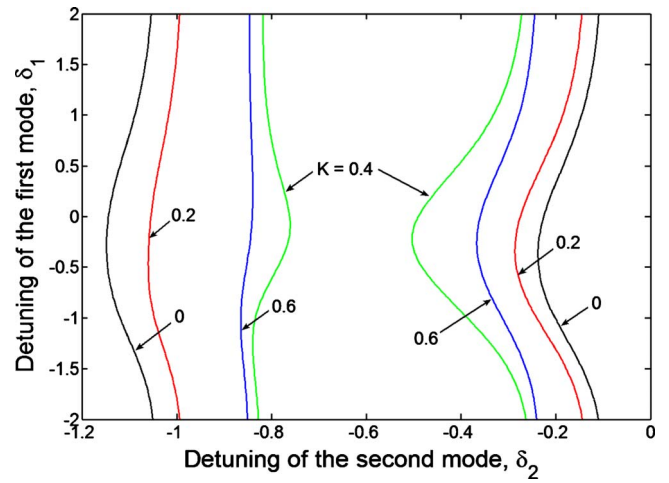


FIG. 8. (Color online) Contours $G_2=10$ of the gain function of the parasitic mode with three variations $q_2=3$ in the plane of detunings δ_1 versus δ_2 for the signal wave amplitude at the entrance $\alpha_{10}=0.1$. Black, red, green, and blue curves show contours for the filling factor equal to 0.0, 0.2, 0.4, and 0.6, respectively.

However, when the parasitic mode has more variations [see Figs. 7(b) and 7(c) for $q_2=2$ and $q_2=3$, respectively] corresponding changes are not so monotonic. For example, in the case of the parasitic mode with two variations shown in Fig. 7(b), the expansion of the beam from $K=0.5$ to $K=0.75$ does not cause significant changes in the gain curve of the second mode because when the beam enters the region of two peaks of this mode the average beam coupling to the parasitic mode does not change significantly. This effect is even more pronounced in the case of the parasitic mode with three variations $q_2=3$ shown in Fig. 7(c). Here, when the beam expansion takes place within the central peak, the increase of the filling factor K reduces the gain function. However, at larger values of the filling factor, i.e., when the beam is expanded in the regions of all peaks, the gain function increases with K [cf. the gain curves for the cases $K=0.5$ and $K=0.75$ in Fig. 7(c)].

The topology of the gain curves in the plane of detunings of both modes is essentially the same as those shown in Figs. 5(a)–5(c). Therefore we will not present them here. Rather, we will illustrate the effect of beam widening on suppression of the parasitic mode by Fig. 8 where the case of the parasitic mode with three transverse variations $q_2=3$ is shown. This case is shown for the input amplitude of the signal wave $\alpha_{10}=0.1$, fixed threshold value of the gain function of the parasitic mode $\langle G_2 \rangle = 10$ and different values of the filling factor K . Initially, the region of excitation of this parasitic mode shrinks as the filling factor increases (cf. this region for zero filling factor with those for $K=0.2$ and 0.4). However, at larger values of the filling factor, as the filling factor increases, the region of parasitic mode excitation widens (cf. this region for $K=0.4$ restricted by green lines with that for $K=0.6$ shown by blue lines) because the beam enters the region of side peaks of the parasitic mode where electrons are coupled to the parasitic mode stronger than to the signal wave.

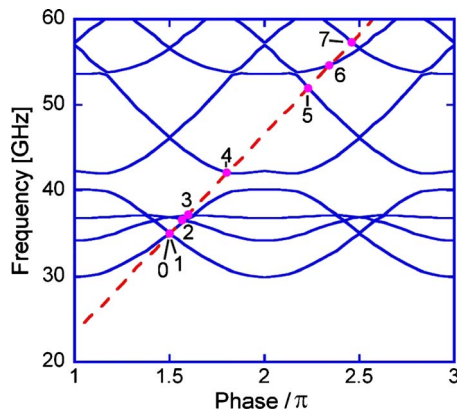


FIG. 9. (Color online) Dispersive characteristics of a sheet-beam coupled-cavity Ka-band slow-wave structure (reproduced from Ref. [30]). (Copyright 2010 IEEE.)

V. DISCUSSION

To illustrate the importance of the problem studied above let us reproduce in Fig. 9 the dispersion diagram for a coupled-cavity slow-wave structure designed for a sheet-beam Ka-band (35 GHz) traveling-wave tube at Naval Research Laboratory [30]. Here the curve 1 is the dispersive curve of the operating forward wave which is surrounded by several parasitic backward waves. The analysis [30] showed that the most dangerous among them are the backward waves 2 and 4 which can be excited near cutoff and whose starting length in the absence of the forward wave is equal to 0.91 and 0.27 inches, respectively. Some possibilities to suppress this parasitic excitation for providing zero-drive stability were analyzed in Ref. [2]. The theory presented above dem-

onstrates the importance of studying in such amplifiers also the effect of the operating forward waves on the excitation of parasitic modes.

It should be noted that the analysis of excitation of parasitic waves in active systems with various types of dispersion can also be of interest for people studying such new problems as the use of metamaterials for high-power microwave applications.

VI. SUMMARY

The theory describing the excitation of parasitic backward waves near cutoff in forward-wave amplifiers is presented. This theory allows one to analyze not only the zero-drive stability, but also the effect of the signal wave on self-excitation conditions of parasitic waves. It is shown that depending on operating parameters not only suppression of parasitic waves by the forward wave, but also their nonlinear excitation (also known as cross-excitation instability) is possible. It is also shown that in amplifiers with a high aspect ratio where electron beams of a sheet configuration are utilized the beam extension in a wide direction may cause various effects depending on the transverse structure of competing forward signal and parasitic backward waves. The fact that the presence of a large amplitude signal wave can greatly modify the region of the parasitic mode self-excitation is especially important for accurate designing of high-power boosters operating in the regime of deep saturation [31].

ACKNOWLEDGMENT

This work was supported by the Air Force Office of Scientific Research.

-
- [1] M. Rosker, *IEEE International Vacuum Electronics Conference*, IVEC-08, Monterey, CA, 2008 (IEEE, Piscataway, NJ 2008).
 - [2] P. Larsen, D. K. Abe, S. J. Cooke, B. Levush, T. M. Antonsen, Jr., and R. E. Myers, *IEEE Trans. Plasma Sci.* **38**, 1244 (2010).
 - [3] G. S. Nusinovich, S. J. Cooke, M. Botton, and B. Levush, *Phys. Plasmas* **16**, 063102 (2009).
 - [4] B. E. Carlsten, *Phys. Plasmas* **9**, 5088 (2002).
 - [5] J. Joe, J. Scharer, J. Booske, and B. McVey, *Phys. Plasmas* **1**, 176 (1994).
 - [6] G. S. Nusinovich, B. Levush, and D. Abe, NRL Memo 6840-03-8673 (March 2003).
 - [7] A. P. Kuznetsov and S. P. Kuznetsov, *Radiophys. Quantum Electron.* **23**, 736 (1980).
 - [8] A. P. Kuznetsov and S. P. Kuznetsov, *Radiophys. Quantum Electron.* **27**, 1575 (1984).
 - [9] L. V. Bulgakova and S. P. Kuznetsov, *Radiophys. Quantum Electron.* **31**, 155 (1988).
 - [10] S. M. Miller, T. M. Antonsen, Jr., B. Levush, A. Bromborsky, D. K. Abe, and Y. Carmel, *Phys. Plasmas* **1**, 730 (1994).
 - [11] G. S. Nusinovich, M. Walter, and J. Zhao, *Phys. Rev. E* **58**, 6594 (1998).
 - [12] K. R. Chu, *Rev. Mod. Phys.* **76**, 489 (2004).
 - [13] G. S. Nusinovich, *Introduction to the Physics of Gyrotrons* (The Johns Hopkins University Press, Baltimore; London, 2004).
 - [14] H. P. Freund and T. M. Antonsen, Jr., *Principles of Free-electron Lasers*, 2nd ed. (Chapman & Hall, London, 1996), p. 7.
 - [15] M. Blank, K. Felch, B. G. James *et al.*, *IEEE Trans. Plasma Sci.* **30**, 865 (2002).
 - [16] E. B. Abubakirov and M. I. Petelin, *Sov. Phys. Tech. Phys.* **33**, 635 (1988).
 - [17] S. N. Vlasov, G. M. Zhislin, I. M. Orlova, M. I. Petelin, and G. G. Rogacheva, *Radiophys. Quantum Electron.* **12**, 972 (1969).
 - [18] L. A. Weinstein, *Radiotekh. Elektron. (Moscow)* **2**, 319 (1957); **2**, 331 (1957).
 - [19] A. Nordsieck, *Proc. IRE* **41**, 630 (1953).
 - [20] R. M. Phillips, *IRE Trans. Electron Devices* **ED-7**, 231 (1960).
 - [21] J. M. J. Madey, *Nuovo Cimento Soc. Ital. Fis., B* **50B**, 64 (1978).
 - [22] G. Caryotakis, in *Modern Microwave and Millimeter-Wave Power Electronics*, edited by R. J. Barker, J. H. Booske, N. C.

- Luhmann, Jr., and G. S. Nusinovich (IEEE-Press; Wiley-Interscience, Piscataway, NJ, 2005), Chap. 3.
- [23] G. Nusinovich, M. Read, and L. Song, *Phys. Plasmas* **11**, 4893 (2004).
- [24] I. G. Zarnitsyna and G. S. Nusinovich, *Radiophys. Quantum Electron.* **17**, 1418 (1974).
- [25] G. S. Nusinovich, *Int. J. Electron.* **51**, 457 (1981).
- [26] B. Levush, T. M. Antonsen, Jr., A. Bromborsky, W. R. Lou, and Y. Carmel, *IEEE Trans. Plasma Sci.* **20**, 263 (1992).
- [27] C. Grabowski, E. Schamiloglu, C. T. Abdallah, and F. Hegeler, *Phys. Plasmas* **5**, 3490 (1998).
- [28] E. A. Gelvich, L. M. Borisov, Y. V. Zhary, A. D. Zakurdayev, A. S. Pobedonostsev, and V. I. Pugin, *IEEE Trans. Microwave Theory Tech.* **MTT-41**, 15 (1993).
- [29] E. R. Colby, G. Caryotakis, W. R. Fowkes, and D. N. Smithe, in *High Energy Density Microwaves*, edited by R. M. Phillips, AIP Conf. Proc. No. 474 (AIP, Woodbury, New York, 1999), p. 74.
- [30] P. B. Larsen, D. K. Abe, S. J. Cooke, B. Levush, and T. M. Antonsen, Jr., *International Vacuum Electronics Conference, IVEC-2010*, Monterey, CA, 2010 (IEEE, Piscataway, NJ, 2010).
- [31] C. R. Smith, C. M. Armstrong, and J. Duthie, *Proc. IEEE* **87**, 717 (1999).